Solid State Sciences 54 (2016) 59–63

Contents lists available at ScienceDirect

Solid State Sciences

journal homepage: www.elsevier.com/locate/ssscie

Photoreflectance investigation of exciton-acoustic phonon scattering in GaN grown by MOVPE

M. Bouzidi [a, c, *], S. Soltani [a, c], I. Halidou [a, b, c], Z. Chine [a, c], B. El Jani [a, c]

[a] Unité de recherche sur les Hétéro-Epitaxies et Applications (URHEA), 5000 Monastir, Tunisia
[b] Département de Physique, Faculté des Sciences et Techniques, Université Abdou Moumouni, BP 10662, Niamey Niger
[c] Université de Monastir, Faculté des Sciences de Monastir, Tunisia

ARTICLE INFO

Article history:
Received 28 August 2015
Received in revised form
1 January 2016
Accepted 4 January 2016
Available online 6 January 2016

Keywords:
GaN
Photoluminescence
Photoreflectance
Exciton linewidth
Acoustic phonon

ABSTRACT

In this paper, we report a systematic investigation of the near band edge (NBE) excitonic states in GaN using low temperature photoluminescence (PL) and photoreflectance (PR) measurements. For this purpose, GaN films of different thicknesses have been grown on silicon nitride (SiN) treated c-plane sapphire substrates by atmospheric pressure metalorganic vapor phase epitaxy (MOVPE). Low temperature PR spectra exhibit well-defined spectral features related to the A, B and C free excitons denoted by FX_A FX_B and FX_C, respectively. In contrast, PL spectra are essentially dominated by the A free and donor bound excitons. By combining PR spectra and Hall measurements a strong correlation between residual electron concentration and exciton linewidths is observed. From the temperature dependence of the excitonic linewidths, the exciton-acoustic phonon coupling constant is determined for FX_A, FX_B and FX_C. We show that this coupling constant is strongly related to the exciton kinetic energy and to the strain level.

1. Introduction

Excitons in wide-gap semiconductors play an important role in optical phenomena since they have a large binding energy and could be stable at room temperature [1–5]. Many researches on excitons in GaN are part of a larger study concerning the development of a new generation of polariton devices based on wide bandgap semiconductor microcavities [4,6,7]. The transport and optoelectronic properties of these devices depend mainly on the vibrational properties of the material, which are influenced by several interactions involving excitons, free carriers, phonons, impurities, and defects [8]. Therefore, the knowledge of such interactions and their influence on the fundamental optical properties of GaN epilayers is crucial for further improvements of the performance of GaN-based optoelectronic devices. For this reason, massive researches have been done over the past decades to understand the scattering mechanism in GaN and particularly the exciton-phonon interaction [4,8–14]. It was found that the temperature dependence of the exciton linewidth provides important information about the dynamics of the exciton-phonon interaction system [8–13]. Surprisingly enough, most of these reports are limited to the FX_A and only little attention was paid to FX_B and FX_C. This can be explained by the lack of high quality materials and proper characterization tools to get such excitonic transitions with high spectral resolution. In fact, in most PL spectra reported so far on GaN, FX_A emission line is dominant, while FX_B and FX_C, under the best circumstances, appear only as a weak shoulder due to its fast decay via nonradiative process [13], and to the excitonic transfer towards the A exciton levels which are located at lower energy. This makes FX_B and FX_C hard to be spectrally resolved and investigated. Furthermore, in the case of reflectance measurement, spectra are dominated by fringes arising from the internal multiple reflections which can engender some errors under the fitting process [12].

Recent advances in growing epitaxial GaN with high quality [15–18] as well as the progress achieved in optical characterization techniques, present the opportunity to study the excitons scattering processes in GaN. In this paper, PR spectroscopy is used to study the scattering properties of free excitons in GaN. The PR spectroscopy was selected because of its high sensitivity, non-destructive nature, and its precision in determining the energy position and the linewidth of optical transition compared to the conventional characterization methods [19]. The results show that the strength of the exciton-acoustic phonon scattering in GaN

* Corresponding author. Unité de recherche sur les Hétéro-Epitaxies et Applications (URHEA), 5000 Monastir, Tunisia.
E-mail address: elbouzidimed16@yahoo.com (M. Bouzidi).

http://dx.doi.org/10.1016/j.solidstatesciences.2016.01.002
1293-2558/

depends strongly on the exciton kinetic energy and on the strain level.

2. Experiments

The investigated GaN layers were grown on c-plane sapphire substrates in a vertical MOVPE reactor equipped with in-situ He–Ne laser reflectometry. Trimethylgallium (TMG) and NH_3 were used as the precursors of gallium and nitrogen, respectively. The carrier gas was a mixture of N_2 and H_2. After a nitridation step at 1080 °C in $NH_3 + N_2 + H_2$ ambient, SiN treatment was carried out by in-situ deposition of a thin SiN mask on the sapphire. The GaN buffer layer and GaN epilayer were grown at 600 °C and 1200 °C, respectively. Details of the process and optimum growth conditions can be found in references [15,16]. The samples used in the present work, were grown under nominally identical conditions except for the thickness which was chosen in such a way that it covers all the different stages of film coalescence process. Table 1 gives the layer thickness, residual electron concentration and Hall mobility of the GaN samples. PL measurements were performed using a 15 mW He–Cd laser working at 325 nm and was detected through a Spectra Pro 2500 monochromator. PR measurements were carried out by employing a standard setup with the 325 nm line of He–Cd laser as the pump light which was mechanically chopped at 280 Hz. The probe light was obtained from a 75 W Xe lamp dispersed with a 275 mm focal length monochromator. The reflected light was dispersed by a 500 mm focal length grating monochromator and was detected using Hamamatsu R-928 photomultiplier.

3. Results and discussions

Fig. 1 displays the low temperature (10 K) PL spectra of samples L1, L3, L4 and L6 normalized according to the NBE maximum peak emission. The PL spectra exhibit donor–acceptor pair (DAP) emissions which is consistent with the results reported in the literature [20,21]. It is clearly observed from Table 1 that the DAP to NBE (DAP/NBE) luminescence intensity ratio decreases as the layer thickness increases and reaches the minimum value (~1/5) for the thickest layer (sample L6). This behavior implies that the density of DAP-related defects decreases with thickness. The DAP peak is commonly attributed to dislocations, residual impurities such as carbon, oxygen and silicon, and intrinsic native defects (gallium and nitrogen vacancies) [16,21]. The high value of DAP/NBE observed for layer L1 is probably due to the high density of oxygen and silicon impurity in the GaN material near the interface region with sapphire (probably due to the out-diffusion from sapphire and from the SiN mask). It can be noted that the ratio DAP/NBE is consistent with the Hall measurements. Indeed, as can be seen by inspecting the data in Table 1, the sample with the highest carrier concentration (and lowest Hall mobility) presents the maximum DAP/NBE ratio, and vice versa. Finally, it should also be noted that the NBE PL spectra at 10 K are largely dominated by the A free (FX_A) and donor bound (D°X) excitonic emissions as shown in the inset of Fig. 1.

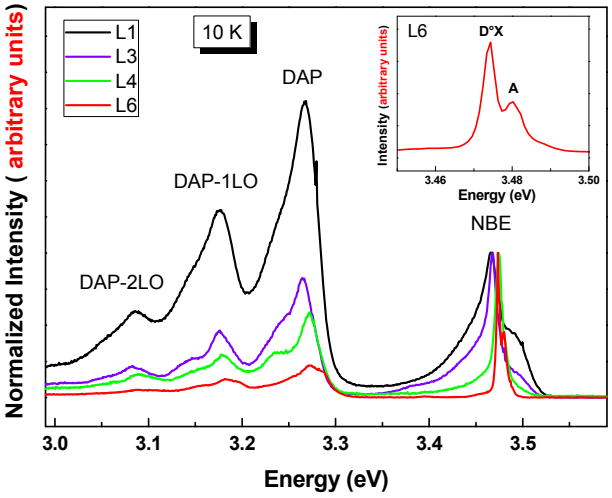

Fig. 1. Low temperature (10 K) photoluminescence spectra of samples L1, L3, L4 and L6. In order to compare the DAP/NBE intensity ratio, the spectra are normalized according to the intensity of the NBE peak. The inset graph shows the emission lines of the excitonic region.

Fig. 2 depicts the PR spectra of the GaN samples measured at 10 K. Contrary to the PL results, PR spectra exhibit well resolved FX_B and FX_C exciton features. Therefore, PR technique is a useful method to investigate the optical properties of all free excitons in GaN epilayers. In order to extract the energies and linewidths of the excitonic transitions, PR spectra were least-square fitted using the third derivative Lorentzian line shape functional form (TDFF) [12,15] given by:

$$\frac{\Delta R}{R} = \mathrm{Re}\sum_{k=1}^{j}\left[A_k e^{i\varphi_k}(E - E_k + i\Gamma_k)\right]^{-m} \quad (1)$$

where, j is the number of the transitions and spectral functions used in the fitting procedure, E is the photon energy, A_k, φ_k, E_k and Γ_k, are respectively, the amplitude, phase, energy and linewidth of the transition k. The exponent m is a characteristic parameter, which equals 2 for excitonic transition. The obtained resonance energies and linewidths of the FX_A, FX_B and FX_C excitons are presented in Table 2. A plot of the excitonic linewidths as a function of electron concentration is shown in Fig. 3. For not degenerately doped layers ($n < 10^{18}$ cm^{-3}), the linewidth of the excitonic transition is almost constant at about 2.5, 2.9 and 4.2 meV for FX_A, FX_B and FX_C, respectively, which is the state of the art for GaN grown on sapphire. However, for degenerately doped layers the linewidth increases with the increase of the electron concentration. As the electron concentration increases from 2×10^{18} to 9×10^{18} cm^{-3}, the exciton linewidth rises from 5 to 2.5 meV for FX_A, from 5.9 to 2.9 meV for FX_B and from 10 to 4.2 meV for FX_C. Many works have

Table 1
Summary of GaN layer thickness, donor–acceptor-pair to the near-band-edge (DAP/NBE) luminescence intensity ratio extracted from PL measurements, residual electron concentration and mobility determined by room temperature Hall effect measurements.

Samples	Thickness (μm)	Electron concentration (cm^{-3})	Mobility (cm^2/V.s)	DAP/NBE ratio
L1	0.3	1.35×10^{19}	36	2.05
L2	0.7	9×10^{18}	60	1.10
L3	0.8	7.6×10^{18}	76	0.82
L4	1.7	3.9×10^{18}	137	0.58
L5	3	2×10^{18}	210	0.25
L6	5	1.5×10^{17}	450	0.22